

A SCALABLE MODEL FOR STIR TANKS

J.L. Ditter and C.W. Hirt
Flow Science, Inc.
December 1993

INTRODUCTION

Mixing vessels are used in the process industry to mix materials together under a variety of thermal and mechanical conditions. These vessels, often referred to as stir-tank reactors, typically contain one or more impellers placed on a central shaft that induce radial and axial flows in the tank [1]. To prevent large scale rotation and induce mixing of the contents, stationary baffles are often placed at the walls of the tank.

Two of the most important aspects of a stir-tank reactor are how well it mixes and the time it takes to mix. Other flow factors of interest are the maximum shear levels in the tank, heat-transfer characteristics, solid suspension capabilities and free-surface motions.

Experience has revealed that it is difficult to scale successful laboratory or intermediate size tanks up to full production sizes [2]. The scaling problem is associated with the fact that it is often impossible to maintain physical similarity in all flow processes when scaling from a laboratory device a few inches in diameter to a full-scale tank that may be many feet in diameter. The scaling problem may also be aggravated by a basic lack of understanding of the mixing mechanisms.

Computer flow modeling appears ripe for application to stir-tank reactors. Indeed, there have been several attempts to model flows in these tanks, some of them showing relatively good comparisons with experimental data [3-6]. In these modeling efforts, however, the impellers have usually been replaced by a specified velocity distribution over the surface of the region carved out by the impeller. The velocity distribution used is taken from measurements made in the experiment. In this sense the models have not been general, nor is it likely they can be accurately scaled up in size.

In particular, if one relies on experimental data for specifying an impeller, it is impossible to predict the effect of a change in the ratio of impeller diameter to the diameter of the tank or what happens when two impellers are moved closer together. In empirically-based models of this sort it is not even possible to predict the consequences of changing the viscosity of the fluid in the tank.

Research efforts are underway in several laboratories to see if the moving blades of an impeller can be directly modeled using some sort of moving-grid numerical scheme, e.g., one based on

the Chimera grid embedding approach [7]. This approach is attractive because it can potentially lead to predictions of detailed secondary flows about the blades. Unfortunately, such a brute force approach is not likely to be useful in the near future because it involves enormous amounts of computer memory and CPU time. Furthermore, to be truly useful, such an approach would have to accurately model boundary layer phenomena in order to predict flow separations from the blades, and it should also resolve the details of fluid instabilities that lead to turbulence. These details are currently at the limit (or well beyond) our present modeling capabilities.

The situation, then, is that a new type of impeller model is needed that has the potential for scaling and that does not require excessive amounts of computer time to produce useful results. This goal is the subject of the current paper. In the next section we describe a simple concept that can be used to construct models of impellers. The approach we propose can be implemented at different levels of detail, depending on the type of impeller involved and the type of information wanted from the simulation.

Comparisons with experimental data for a single pitched-blade impeller are used to verify the usefulness of our proposed model. We conclude our presentation with several illustrations of how this new model can be used in practical situations.

A NEW IMPELLER MODEL

The rotating blades of an impeller push on the surrounding fluid imparting net momentum to the fluid in one or more directions. Combining this observation with the fact that mixing times are usually very long compared to the time it takes for an impeller to make one rotation, we are led to consider an impeller model as some sort of momentum source distributed over the region swept out by the impeller blades.

Construction of Momentum Source

The simplest momentum source is one proportional to the difference between the blade velocity and the fluid velocity,

$$\text{Fluid Momentum Change} = K \left(\vec{U}_b - \vec{U} \right), \quad (1)$$

where a subscript "b" indicates the blade velocity, and K is a "drag" or "accommodation" coefficient. In general, K is a function of space and time.

We may make this suggestion plausible in the following way. Immediately at the surface of a blade the fluid must have the same velocity as the blade. We can insure this velocity boundary condition at the blade using the proposed momentum term, Eq.1, if we make K a delta function [8]; that is, if we make K a function whose value is zero everywhere except at the surface of the

blade, where its value is infinite. The infinite value must be chosen such that a spatial integration of the fluid momentum equation with the K term included leads to the result $\vec{U} = \vec{U}_b$ at the blade surface. In this limit, then, Eq.1 can be used to satisfy the correct boundary condition on the moving blade.

In practice, of course, we cannot deal with ideal delta functions in a discrete numerical approximation. The function must be spread over a spatial distance of at least one volume unit (i.e., mesh cell in a finite-difference or control volume method). If we spread the function out over a greater region, its magnitude must decrease such that the spatial integral over the entire function has a constant value.

Now we can imagine an impeller with N blades, each of which is represented by a smoothed delta function. The limiting case of complete smoothing would be a uniform value of K spread over the disk swept out by the blades. This, in fact, is the simplest representation of our proposed impeller model. Only in cases where the number of blades is small and they are moving slowly would it seem reasonable to retain the spatial and time-dependence of the individual blade K values.

There is one refinement to Eq.1 that must be considered. As it stands, the proposed model will try to make both normal and tangential fluid velocities conform to the specified blade motion. In high Reynolds number situations the momentum imparted to the fluid will be mostly through form-drag effects and not because of viscous forces. In this limit we should only be imposing momentum changes associated with velocities normal to the impeller blades and should not add momentum changes in directions tangent to the blade surfaces. In this case, then, we must modify Eq.1 to have the form,

$$\text{Normal Momentum Change} = K \left[\vec{U}_b - \left(\vec{U} - \vec{U}_t \right) \right], \quad (2)$$

where \vec{U}_t is the component of fluid velocity tangent to the blade (and \vec{U}_b is assumed to be a normal velocity). The principal difference between Eq.1 and Eq.2 is that the first equation may retard some radial flow in the impeller disk region. The quantitative significance of this remains to be investigated.

Specification of Blade Velocities

To complete our model, it is necessary to specify the blade velocity, \vec{U}_b . For this purpose we assume the azimuthal velocity, U_{rot} , is equal to the rotation velocity of the blade,

$$U_{rot} = \Omega R, \quad \text{for } R_{in} < R < R_{out}.$$

where Ω is the impeller rotation rate in radians-per-second and R is the radial distance from the axis of rotation. This relation is limited to R values between an inner radius, R_{in} and an outer radius R_{out} . The outer radius equals the radius of the impeller, while the inner radius depends on whether or not the blades extend all the way to the axis or terminate at the edge of a hub. Note that the sign of Ω can be used to specify the sense of rotation (i.e., clockwise or counter clockwise).

Axial velocities, U_{ax} , are also assumed to be proportional to the rotation velocity, but with a multiplicative constant A ,

$$U_{ax} = A\Omega R \quad \text{for } R_{in} < R < R_{out}.$$

Thus, purely radial impellers would be assigned $A=0$, while pitched-blade impellers have non-zero A values. The sign of A can be used to direct the axial flow up or down.

If the impeller has a hub that blocks axial flow, this is best modeled by an obstacle but may also be approximated by making the axial velocity equal to zero where R is less than the hub radius.

In its simplest form, then, our impeller model is specified by the five parameters:

- K = accommodation coefficient
- Ω = rotation rate in radians per second
- A = ratio of axial to azimuthal velocity
- R_{in} = inner radius of blades or hub radius
- R_{out} = diameter of impeller

The most important parameter K is a function of space since it is non-zero only in the region swept out by the blades. We expect that K will certainly be proportional to the number of blades in the impeller. Most probably it should also be a weak function of such things as blade shape, viscous effects, etc.

Comparison with Test Data

To test the new model we have made comparisons with the experimental data of Jaworski, et al [9]. Their test consisted of a single 45° pitched-blade impeller in a right-circular tank. The impeller had six blades with a diameter equal to one third the diameter of the tank. The tank was filled with water to a depth equal to its diameter. Four radial baffles having a width of one tenth the tank diameter were located at the tank wall with 90° spacing. Two test configurations were studied: one with the impeller at mid height in the tank and the other with the impeller placed one fourth of the height up from the bottom. The existence of these two cases was considered especially valuable for validation purposes. Figures 1A-1B, reproduced from Ref. 9, show the measured velocity distributions for the two cases.

Our impeller model was inserted in the commercial fluid dynamics solver FLOW-3D developed by Flow Science, Inc. [10]. The numerical representation of the tank consisted of a nearly uniform rectangular mesh 22 by 22 cells in the horizontal (x-y) plane and 30 cells axially. The cylindrical tank was cut out of the mesh using the fractional area/volume method FAVOR; see mesh plot in Fig.2. Using a rectangular mesh rather than a cylindrical one has the advantage of eliminating the singular point at the cylindrical axis and provides more uniform gridding over the entire flow region.

For our tests we chose the momentum term in Eq.1 with K equal to 10, the number of revolutions per second. This number was a guess based on a few preliminary calculations for a different tank that had no experimental data available for comparisons. For the ratio of axial to azimuthal velocity, a value of $A=1.5$ was selected on the basis of experimental observations made by Ranade and Joshi [3].

We used the viscous blade model, Eq.1, for simplicity even though the calculations were performed under the assumption of negligible fluid viscosity and wall-shear effects (because Reynolds numbers were of order 24,000). This choice incorrectly reduced radial flow in the impeller disk region but should not introduce major errors in the overall results.

Figures 3A-3B show the computed flow fields in a vertical plane offset from the axis by one half mesh cell. The left-right asymmetry is caused by this offset -- overlaying plots from opposite sides of the axis shows that the visually averaged flow is symmetric in the plane containing the axis.

Qualitatively, the computed flows are in excellent agreement with the observations, Fig.1A-1B. For example, there are large reverse (upward) core flows under the impeller, strong downward flows under the outer portion of the impeller blades and narrow, but strong, upward flows along the outside wall of the tank. Vortex center positions are accurately reproduced. The biggest discrepancy is in the mid-height case where observations show that the reverse flow core extends over the entire bottom of the tank, while in the computation it only extends over about half the bottom.

Quantitatively, the computed results are also in good agreement with the data. For instance, in the mid-height case the computed maximum axial velocity was 50 cm/s compared to a measured 54 cm/s. The computed maximum radial velocity was 18 cm/s while the measured value was about 23 cm/s. Both of these values are within the reported experimental reproducibility range of plus or minus 6.12 cm/s.

For the lower impeller position, the maximum axial velocity was stated in the text of Ref. 9 to be about 67 cm/s, but the plotted data (Fig.4 of Ref. 9) indicates that this value is closer to 46 cm/s. The maximum radial velocity was measured to be 38 cm/s. Our computations gave a maximum axial velocity of 49 cm/s and maximum radial velocity of 35 cm/s. Both values are well within the experimental reproducibility limits. Upward flow velocities along the tank side wall were 38 cm/s in the experiment and the simulation.

Both impeller locations were computed using the same model parameters. This lends support to the ability of the new model to adjust to changing geometric conditions, hence to its potential for accurate scaling. More comparisons with experiments are certainly needed to ascertain the dependence of parameters K and A on impeller design (e.g., number and shape of blades). Nevertheless, these results are extremely encouraging and, as the next section will demonstrate, the new model has considerable potential for modeling detailed flow phenomena in mixing tanks.

ILLUSTRATIVE APPLICATIONS

To illustrate how the present impeller model might be used to improve the design of a mixing vessel, we first look at the effect of changing impeller types in a two-impeller tank. Second, we illustrate how the new model can easily be generalized by considering an approximation to a Phaudler vessel in which the impeller blades are modeled by a more sophisticated time- and space-dependent accommodation coefficient.

A Two Impeller Tank

Consider a typical tank configuration as shown in Fig.4. This tank -- 68 inches in diameter and 116 inches high -- has an elliptical bottom and contains liquid to a depth of 108 inches. There are two impellers: a pitched-blade impeller located 80 inches above the tank bottom and a radial impeller 22 inches above the bottom. Both impellers are rotating at 100 rpm.

Our numerical simulation of this tank, which resulted in Fig.4, used the same accommodation coefficient $K=1.67$ for both impellers (1.67 is the number of revolutions per second, the same prescription as used in the previous section). For the pitch-blade impeller the ratio of axial to azimuthal velocity was specified to be $A=1.5$, while $A=0$ was used for the radial impeller.

As can be seen from Fig.4, the impellers are not effective in mixing the entire contents of the tank. In particular, the lower half of the tank is experiencing little mixing with fluid in the upper regions. To explore possible remedies, a computational experiment was performed in which the lower, radial impeller was replaced with a second pitched-blade impeller.

After computing the results to a problem time of 50 s, Fig. 5, it appeared that the combination of two pitch-blade impellers was considerably more effective in mixing the contents at all levels.

Continuing the computation beyond 50 s, however, revealed a new phenomenon not observed in earlier calculations. The flow in the tank undergoes a transition that introduces a slow precession about the tank's axis with a period of 8.56 s (equal to about 14.3 impeller revolutions). Furthermore, where there was 90° symmetry before the transition, the symmetry drops to 180° afterwards. This transition is clearly shown in the computed results at 80 s given in Fig. 6.

An idea of the transition and subsequent flow periodicity can be seen in the vertical-velocity history plot taken near the outside edge of the lower impeller. This type of slow precession

model other types of flow agitators besides impellers.

REFERENCES

1. David S. Dickey, "Succeed at Stirred-Tank-Reactor Design," Chem. Eng. Prog., p.22, December 1991.
2. Douglas E. Leng, "Succeed at Scale Up," Chem. Eng. Prog., p.23, June 1991.
3. V.V. Ranade and J.B. Joshi, "Flow Generated by Pitched Blade Turbines II," Chem. Eng. Comm. 81, 225 (1989).
4. V.V. Ranade and J.B. Joshi, "Flow Generated by a Disc Turbine: Part II," Trans. IChemE, 68, 34 (1990).
5. S.M. Kresta and P.E. Wood, "Prediction of the Three-Dimensional Turbulent Flow in Stirred Tanks," AIChE Jour. 37, 448 (1991).
6. A.D. Gosman, C. Lekakou, S. Politis, R.I. Issa and M.K. Looney, "Multidimensional Modeling of Turbulent Two-Phase Flows in Stirred Vessels," AIChE Jour. 38, 1946 (1992).
7. J.A. Benek, P.G. Buning and J.L. Steger, "A 3-D Chimera Grid Embedding Technique," AIAA paper 85-1523, AIAA 7th Computational Fluid Dynamics Conf., Cincinnati, Ohio, July (1985).
8. M.J. Lighthill, Fourier Analysis and Generalised Functions, Cambridge Uni. Press, London (1958).
9. Z. Jaworski, A.W. Nienow, E. Koutsakos, K. Dyster and W. Bujalski, "An LDA Study of Turbulent Flow in a Baffled Vessel Agitated by a Pitched Blade Turbine," Trans. IChemE 69, 313 (1991).
10. R.P. Harper, C.W. Hirt and J.M. Sicilian, "FLOW-3D: Computational Modeling Power for Scientists and Engineers," Flow Science, Inc. report FSI-91-001 (1991).

Note:

An abbreviated version of this paper, under a slightly different title, is to be presented at the Forum on Industrial and Environmental Applications of Fluid Mechanics, 1994 ASME Fluids Engineering Division Summer Meeting, Incline Village, Nevada, June 19-23, 1994.

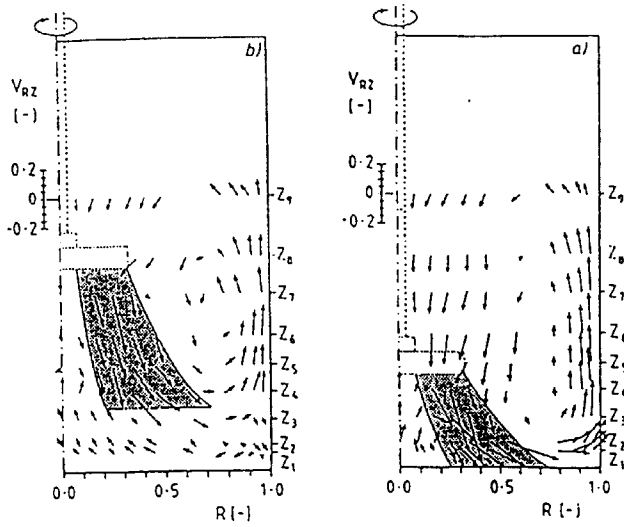


Fig. 1. Experimental results duplicated from Ref.9. Upper impeller position on left and lower position on right.

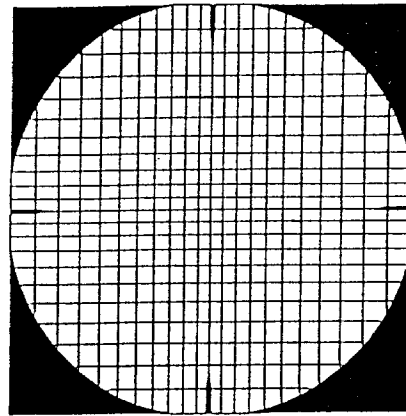


Fig. 2. Horizontal plane showing grid with tank and baffles shaded.

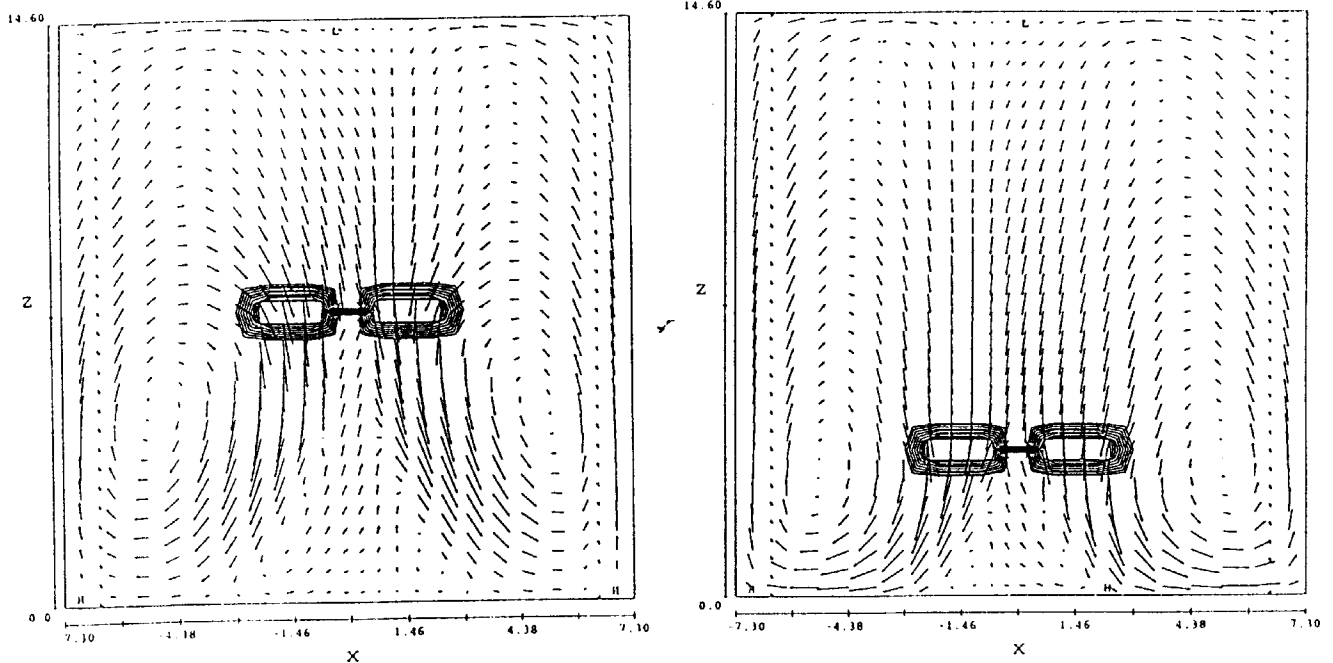


Fig. 3. Computed flow fields for upper impeller position on left and lower position on right. Impeller disk region is defined by contours of a function of the accommodation coefficient.

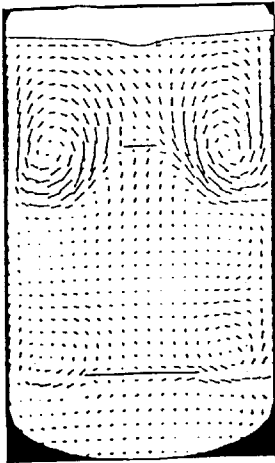


Fig. 4. Flow generated with upper pitched-blade impeller and lower radial impeller. Poor mixing is observed.

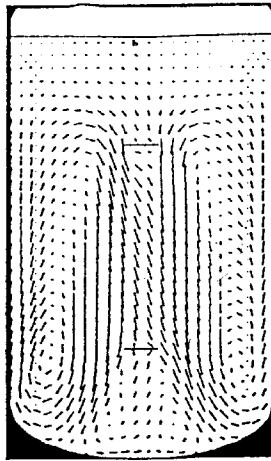


Fig. 5. Flow generated by two pitched-bladed impellers at $t=50s$. Horizontal cross section is near top of fluid. Good mixing exists over most of the vessel.

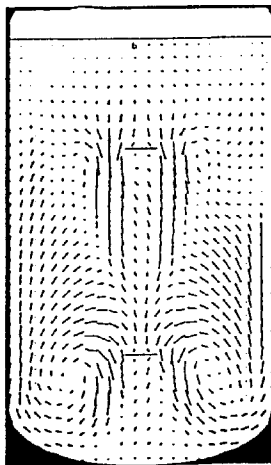
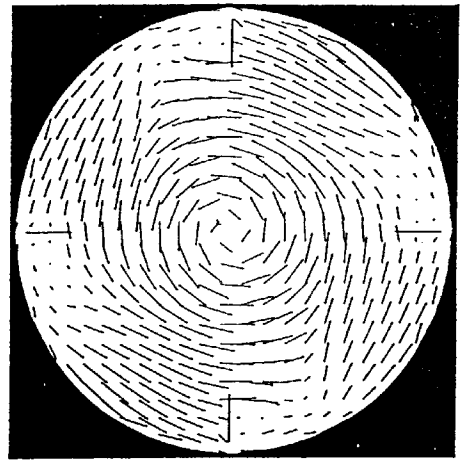


Fig. 6. Flow generated by two pitched-bladed impellers at $t=80s$, after transition to a precessing flow. Comparison with Fig. 5 shows reduction in azimuthal periodicity.

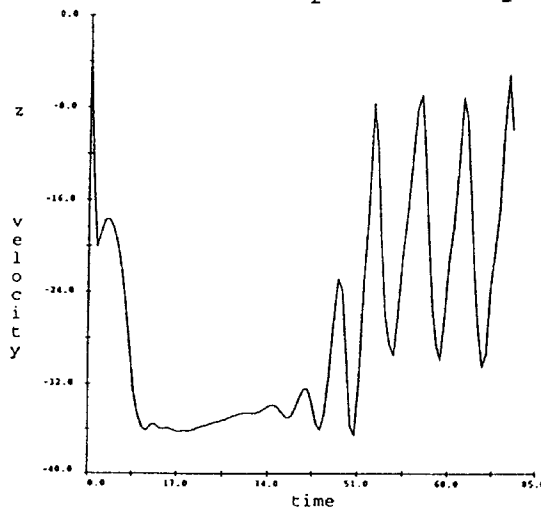
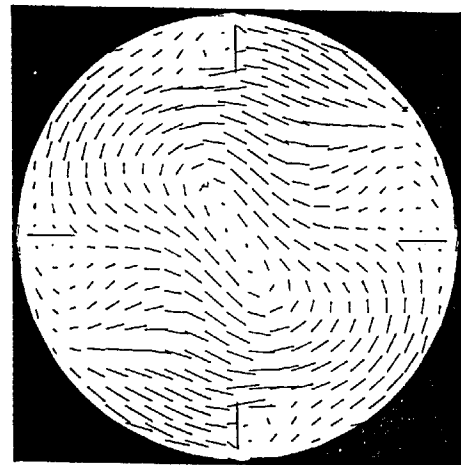


Fig. 7. Time history of vertical velocity near outer edge of lower impeller showing transition to periodic flow.

